RESEARCH ARTICLE

Hsa_circ_0023179 modulated the processes of proliferation, apoptosis, and EMT in non-small-cell lung cancer cells via the miR-615-5p/CDH3 axis

Qingkui Guo ⦿*, Min Zheng ⦿, Chen Zhu ⦿, and Bin Wu ⦿

Circular RNA (circRNA) has been widely studied as a competitive endogenous RNA targeting microRNA (miRNA)/messenger RNA to regulate cancer progression. However, the regulatory mechanism of circ_0023179 in non-small-cell lung cancer (NSCLC) remains unclear. The expression levels of circ_0023179, miR-615-5p, and Cadherin 3 (CDH3) in NSCLC were detected using quantitative real-time polymerase chain reaction. The stability of circ_0023179 was verified using ribonuclease R enzyme, Actinomycin D and agarose gel electrophoresis. Colony formation and thymidine analog 5-ethynyl-2'-deoxyuridine assays were performed to examine proliferation changes in NSCLC cells. Western blot was used to assess the levels of CDH3 and epithelial–mesenchymal transition (EMT)-related marker proteins to evaluate EMT. Dual-luciferase reporter, RNA immunoprecipitation (RIP), and RNA pull-down assays were performed to explore the potential mechanisms of circ_0023179 in regulating NSCLC progression. Finally, the effects of circ_0023179 on NSCLC tumor growth in vivo were explored using a nude mouse subcutaneous tumor model. The results showed that the expression of circ_0023179 was remarkably higher in NSCLC tissues and cells, and it had a significant effect on NSCLC cell proliferation. Additionally, the knockdown of circ_0023179 significantly inhibited tumor growth in NSCLC mice. Mechanistically, circ_0023179 alleviated its inhibition of downstream CDH3 through the sponge-like adsorption of miR-615-5p. The downregulation of miR-615-5p and the upregulation of CDH3 mitigated the inhibitory effect of silencing circ_0023179 on NSCLC cell proliferation. In conclusion, silencing circ_0023179 inhibited NSCLC cell proliferation by targeting the miR-615-5p/CDH3 axis involved in NSCLC progression.

Keywords: Non-small-cell lung cancer (NSCLC), circ_0023179, Cadherin 3 (CDH3).

Introduction

Lung cancer is a malignancy with high cancer-related mortality rates worldwide [1]. Non-small-cell lung cancer (NSCLC), a heterogeneous tumor, accounts for approximately 85% of all newly diagnosed lung cancers [2, 3]. Although treatments for NSCLC are being explored, the prognosis for patients remains poor. Therefore, identifying potential molecular targets is crucial for improving the diagnosis and prognosis of NSCLC.

Circular RNA (circRNA) is a unique, continuous, covalently closed-loop structure that lacks a 5' cap and 3' tail [4]. CircRNA is widely expressed in the cytoplasm and plays an integral role in the progression of various human cancers, including NSCLC [5, 6]. For instance, Circ_0000079 competitively binds to FXR1, inhibiting the formation of the FXR1-protein kinase C iota complex, thereby preventing cell invasion in NSCLC [7]. Wang and Li [8] demonstrated that silencing circ_0067934 inhibited NSCLC cell viability and impacted NSCLC prognosis. Previous studies have also indicated that the high expression of circ_0023179 in NSCLC is associated with histological type, TNM stage, lymph node metastasis, and distant metastasis. Compared with traditional tumor markers, circ_0023179 exhibits higher sensitivity and specificity, suggesting its potential as a biomarker for NSCLC [9]. However, the downstream regulatory mechanism of circ_0023179 in NSCLC progression remains unclear.

MicroRNAs (miRNAs) typically play a regulatory role in cancer development by targeting messenger RNAs (mRNAs) [10]. Studies have confirmed that miR-615-5p functions as a tumor suppressor in various cancers. For instance, miR-615-5p regulates the tumorigenicity of hepatocellular carcinoma (HCC) by negatively affecting oncogene levels, such as those of the insulin-like growth factor 1 receptor, serine hydroxymethyl-transferase 2, and hydroxyacid oxidase 2 [11–13]. Additionally, miR-615-5p is regulated by circ_002144, which suppresses colorectal cancer metastasis by down-regulating La ribonucleoprotein 1 [14]. Furthermore, several studies have shown that circ_100146, circ_0004396, and LINC00324 act as sponges for miR-615-5p, thereby influencing the biological characteristics of NSCLC cells [15–17]. However, it remains unknown whether

circ_0023179 regulates miR-615-5p to modulate NSCLC progression.

Cadherin 3 (CDH3), also known as P-cadherin, plays a key role in cell growth [18]. CDH3 is overexpressed in various cancers, including thyroid, pancreatic, and HCCs and is associated with a poor clinical prognosis [19–21]. However, its function in NSCLC is still unclear. In this study, we aimed to investigate the changes in the levels of circ_0023179, miR-615-5p, and CDH3 in NSCLC, as well as to elucidate their interactions using bioinformatics tools and relevant experimental methods. Specifically, this study aimed to demonstrate that circ_0023179 influences NSCLC progression through the miR-615-5p/CDH3 axis.

Materials and methods

Clinical tissue samples
A total of 45 NSCLC tissues and paired normal tissues were obtained from Tongren Hospital, Shanghai Jiao Tong University School of Medicine. All NSCLC patients provided informed consent. The study procedures were approved by the Ethics Committee of Tongren Hospital, Shanghai Jiao Tong University School of Medicine.

Cell culture and cell transfection
Human NSCLC cell lines (A549, H520, H1299, and H1975) and human bronchial epithelial (HBE) cells (Cell Bank of Chinese Academy of Sciences, Shanghai, China) were maintained in Dulbecco's Modified Eagle Medium (Invitrogen, Carlsbad, CA, USA) supplemented with 10% foetal bovine serum and 1% penicillin/streptomycin in a 5% carbon dioxide (CO_2) incubator at 37 °C. The cells grown in the logarithmic proliferation phase were transfected with corresponding sh-NC, sh-circ_0023179, anti-miR-NC, anti-miR-615-5p, vector and CDH3 according to Lipofectamine 2000 reagent (Invitrogen) instructions. The plasmids and vectors were synthesized by GenePharma (Shanghai, China). Transfected cells were cultured for 48 h before being used for subsequent experiments.

Quantitative real-time polymerase chain reaction (qRT-PCR)
Total cellular RNA was extracted using TRIzol reagent (Invitrogen), and complementary DNA (cDNA) was synthesized using the QuantiTect Reverse Transcription Kit (DXT-205314; Qiagen, Valencia, CA, USA). The cDNA was quantified using the QuantiTect SYBR Green PCR Kit (XT-204143; Qiagen) on an ABI7300-Fast qRT-PCR system (Applied Biosystems, Foster City, CA, USA). Relative quantification of the target genes was analyzed using the $2^{-\Delta\Delta Ct}$ method with glyceraldehyde-3-phosphate dehydrogenase (GAPDH) and U6 as internal references. Primer sequences: U6: F: 5′-CTCGCT TCGGCAGCACAT-3′; R: 5′-TTTGCGTGTCATCCTTGCG-3′; GAP DH: F: 5′-GTCTCCTCTGACTTCAACAGCG-3′; R: 5′-ACCACCC TGTTGCTGTAGCCAA-3′; circ_0023179: F: 5′-GGACACCAACAT GATCGAGTCG3′; R: 5′CGCTCAATGCTGTGCAGATTCC-3′; miR-615-5p: F: 5′-TCCCCGGTGCTCGGA-3′; R: 5′-GAACA TGTCTGCGTATCTC-3′; CDH3: F: 5′-CAGGTGCTGAACATCACG GACA-3′; R: 5′-CTTCAGGGACAAGACCACTGTG-3′.

CircRNA validation
First, 5 μg of RNA was taken. Next, 2 μL of ribonuclease (RNase) R 10X Reaction Buffer, 0.5 μL of RNase R (10U, Sigma-Aldrich, St. Louis, MO, USA), and RNase-Free water were added to make a total volume of 20 μL. The mixture was centrifuged and digested at 37 °C for 30 min, then purified using a column. Transcription was inhibited by adding Actinomycin D (Act D; 2 mg/mL; Sigma-Aldrich) to the NSCLC cell culture medium for 0, 6, 12, and 24 h. The expression of circ_0023179 and LRP5 was then detected by qRT-PCR.

Western blot analysis
Cells were lysed using radioimmunoprecipitation assay lysis buffer (Beyotime, Shanghai, China). Electrophoresis was performed with 12% sodium dodecyl-sulfate polyacrylamide gel electrophoresis, and the proteins were then transferred to polyvinylidene fluoride membranes (Millipore, Billerica, MA, USA). The membranes were incubated with primary antibodies (dilution at 1:1000, Abcam, Cambridge, MA, USA) against N-cad (ab76011), Snail1 (ab216347), E-cad (ab231303), CDH3 (ab242060), and GAPDH (ab8245) at 4 °C for 24 h. Secondary antibodies (1:5000 dilution) conjugated with horseradish peroxidase were applied for 2 h at 37 °C. Protein bands were detected by chemiluminescence using a Tanon 5200 chemiluminescence gel imaging system (Tennant, Shanghai, China).

Colony formation assays
After cell digestion and centrifugation, the cells were counted. Next, 5 mL of medium was added to each well, which contained 1000 cells, and the cells were evenly distributed at the bottom of the six-well plate. The cells were incubated in a 5% CO_2 incubator at 37 °C. The medium was changed every 3–5 days. After 5 days, the cell growth status was observed daily. Depending on the cells, fixation and staining began after 7–14 days when each colony was larger than 50 cells. Pictures were taken with a camera (Nikon, Tokyo, Japan), and ImageJ was used to analyze the results and count the number of colonies.

EdU assays
The cells (1×10^5 cells/well) were inoculated into 96-well plates and incubated at 37 °C for 24 h. After PBS washing, 10 μM EdU culture medium was added and incubated for 1 h in the dark. The cells were washed with PBS, fixed with 4% paraformaldehyde for 15 min at room temperature, and permeabilized with PBS containing 0.3% Triton X-100 (X100, Sigma-Aldrich) for 10 min. The Click reaction solution was incubated in the dark for 30 min, and the DAPI dye solution (D9542, Invitrogen) was then added to stain the nucleus for 10 min. After anti-quenching, the cells were observed with an IX73 fluorescent microscope (Olympus, Tokyo, Japan) at a magnification of 200×.

RNA pull-down assays
The A549 and H1299 cells were transfected with biotin-labeled miR-615-5p (Bio-miR-615-5p) and a negative control (Bio-miR-NC), respectively. After 48 h, the cells were lysed, the supernatant was collected, and magnetic beads labeled with streptavidin were added and mixed. The levels of circ_0023179

Guo et al.
circ_0023179 modulates NSCLC
156
www.biomolbiomed.com

in the RNA complexes bound to the beads were then measured by qRT-PCR.

RIP assays

A Magna RNA immunoprecipitation (RIP) kit (Millipore) was used to enrich circ_0023179 and miRNA. The cells were lysed with RIP lysis buffer, and 100 μL of whole cell extract was treated with magnetic beads containing a circ_0023179 antibody at room temperature for 2 h. Subsequently, the samples were washed with RIP washing buffer and treated with proteinase K at 55 °C for 30 min to isolate RNA-protein complexes from the magnetic beads. qRT-PCR was used to detect target circRNA and miRNA.

Dual-Luciferase reporter assays

Wild-type (WT) circ_0023179/CDH3 and mutant (MUT) circ_0023179/CDH3 were PCR-amplified and inserted into the pmirGLO reporter vector in the following order: circ_0023179$_{wt}$, circ_0023179$_{mut}$, CDH3 3′UTR$_{wt}$, CDH3 3′UTR$_{mut}$. Subsequently, circ_0023179$_{wt}$ and miR-NC, circ_0023179$_{wt}$ and miR-615-5p mimics, circ_0023179$_{mut}$ and miR-NC, circ_0023179$_{mut}$ and miR-615-5p mimics, CDH3 3′UTR$_{wt}$ and miR-NC, CDH3 3′UTR$_{wt}$ and miR-615-5p mimics, CDH3 3′UTR$_{mut}$ and miR-NC, and CDH3 3′UTR$_{mut}$ and miR-615-5p mimics were co-transfected into the A549 and H1299 cells, respectively, using Lipofectamine 2000. Cells were collected after 48 h of incubation, and luciferase activity was detected using the Dual-Luciferase Reporter Assay System (Promega, Madison, WI, USA).

A total of ten male BALB/c nude mice (aged four weeks) were obtained from Beijing Viton Lever Laboratory Animal Technology Co., Ltd. All mice were housed under specific pathogen-free conditions and maintained in a laminar flow cabinet. The mice were then divided into the sh-NC and sh-circ_0023179 groups (with five mice per group). A549-sh-NC and A549-sh-circ_0023179 cells were injected through the skin into the BALB/c nude mice. Tumor size was recorded weekly by measuring the tumor length and width, and the volume was calculated as follows: volume = (length × width^2)/2. After four weeks, the nude mice were sacrificed, tumor tissues were collected and tumor volume was measured and weighed. All procedures were approved by the Ethics Committee of Tongren Hospital, Shanghai Jiao Tong University School of Medicine. The tumor tissues were divided into two parts: one part was fixed with 4% paraformaldehyde and paraffin-embedded to prepare tissue sections for immunohistochemical (IHC) staining of Ki-67, and the positive expression of Ki-67 was analyzed using ImageJ software. The other part was used to obtain RNA and related marker proteins from the tumor tissue.

Ethical statement

The study procedures were approved by the Ethics Committee of Tongren Hospital, Shanghai Jiao Tong University School of Medicine.

Statistical analysis

All experiments were independently repeated at least three times. Statistical analysis was performed using GraphPad Prism 5.0, and data are expressed as the mean ± standard deviation. Differences between multiple groups were analyzed using one-way analysis of variance. The Student's *t*-test was used to compare differences between two independent groups. A *P* value < 0.05 was considered statistically significant.

Results

Circ_0023179 was stably hyper-expressed in NSCLC

Research has reported that LRP5 plays a role in regulating the prognosis of multiple cancers, including NSCLC [22, 23]. Furthermore, the action of circRNA is closely linked to the action of its corresponding mRNA, as circRNA is derived from the reverse splicing of the precursor mRNA. The reverse splice site of circ_0023179 in its corresponding mRNA, LRP5, and its loop structure are shown in Figure 1A. Circ_0023179 was further analyzed to confirm its high expression in NSCLC tissues (see Figure 1B). The expression of circ_0023179 in four NSCLC cell lines was measured, revealing that circ_0023179 was most highly expressed in the A549 and H1299 cells (see Figure 1C). Additionally, circ_0023179 was resistant to RNase R digestion, while LRP5 was largely digested by RNase R (see Figure 1D and 1E). Similarly, the Act D assays confirmed the stability of circ_0023179 (see Figure 1F and 1G). Subsequently, nucleic acid electrophoresis was used to verify the PCR products of the cDNA and gDNA of circ_0023179, with the 379 bp gDNA being detected (see Figure 1H and 1I).

Knockdown of circ_0023179 inhibits NSCLC proliferation and epithelial–mesenchymal transition (EMT)

Preliminary assays showed that circ_0023179 was optimally expressed in NSCLC cells. Consequently, circ_0023179 was selected for knockdown in two cell lines (A549-sh-circ_0023179 and H1299-sh-circ_0023179) to generate stable knockdown cell lines (see Figure 2A). Flat-plate clonogenesis assays revealed that sh-circ_0023179 decreased the number of clonal cells in NSCLC cells (see Figure 2B). Similarly, the EdU results showed that sh-circ_0023179 inhibited NSCLC cell proliferation (see Figure 2C). Additionally, after circ_0023179 knockdown, the expression of N-cad and Snail1 proteins decreased, while the expression of E-cad protein increased (see Figure 2D and 2E).

Circ_0023179 sponge-like adsorption of MiR-615-5p

Potential miRNAs predicted to interact with circ_0023179 using biological databases included miR-615-5p and miR-623 (Figure 3A). RIP was performed with a circ_0023179 probe in A549 and H1299 cells, revealing that miR-615-5p was significantly enriched (see Figure 3B and 3C). Figure 3D shows the predicted binding sites of circ_0023179 to miR-615-5p. MiR-615-5p was lowly expressed in NSCLC tissues and cells (see Figure 3E and 3F). Furthermore, miR-615-5p mimics were co-transfected with luciferase plasmids containing circ_0023179 WT and MUT sequences into NSCLC cells, and miR-615-5p was found to significantly reduce the luciferase activity of circ_0023179 WT but not circ_0023179 MUT (see Figure 3G and 3H). The miR-615-5p pull-down assays also showed that circ_0023179 was considerably enriched (see Figure 3I and 3J).
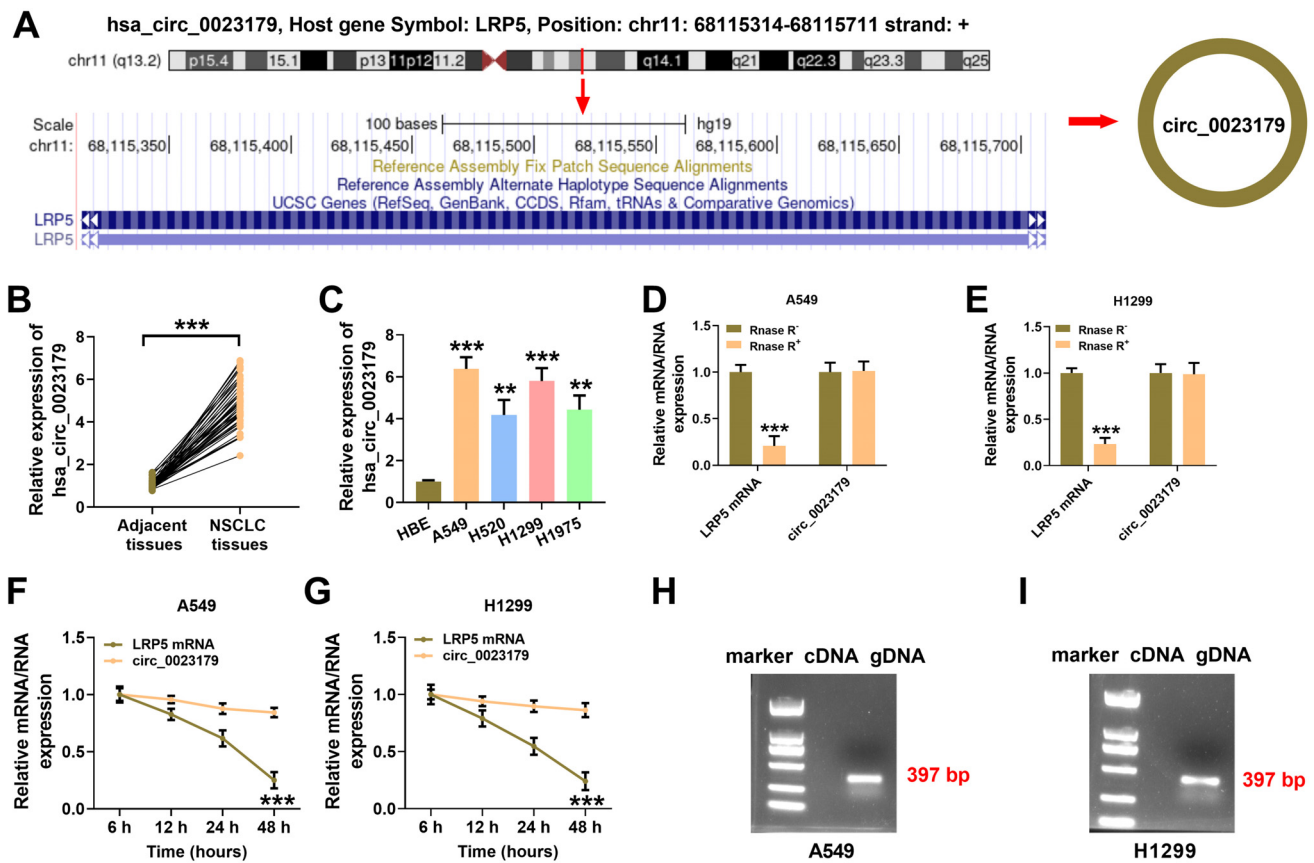
Figure 1. Circ_0023179 was highly expressed in NSCLC. (A) Schematic diagram of the structure of circ_0023179; (B) qRT-PCR was used to detect the expression of circ_0023179 in NSCLC tissues and paraneoplastic tissues; (C) qRT-PCR was used to detect the expression of circ_0023179 in HBE cells and four NSCLC cell lines (A549, H520, H1299, and H1975); (D and E) qRT-PCR was used to detect circ_0023179 and LRP5 in A549 and H1299 cells treated with RNase R; (F and G) qRT-PCR was used to detect circ_0023179 and LRP5 in A549 and H1299 cells treated with actinomycin D; (H and I) Nucleic acid electrophoresis was used to verify the PCR products of the cDNA and gDNA transcripts of circ_0023179. *P < 0.05, **P < 0.01, ***P < 0.001. NSCLC: Non-small-cell lung cancer; qRT-PCR: Quantitative real-time polymerase chain reaction; HBE: Human bronchial epithelial; cDNA: Complementary DNA.
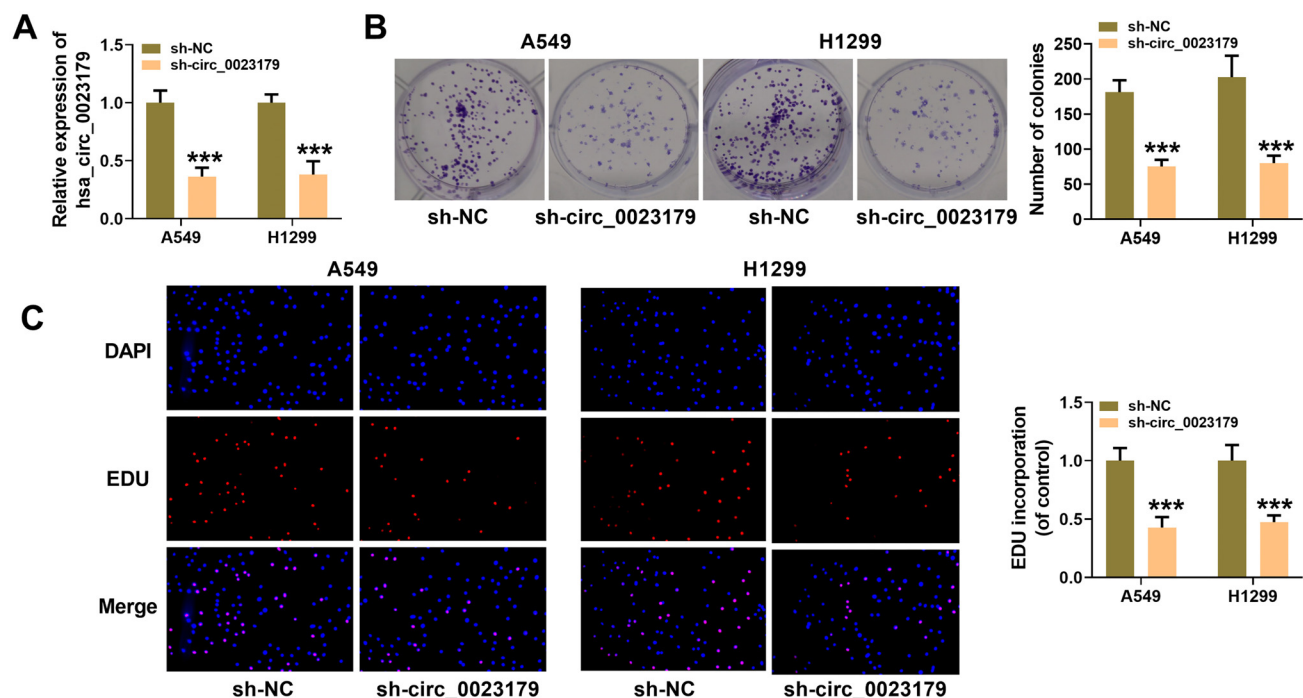
Figure 2. Continued on next page

Guo et al.
circ_0023179 modulates NSCLC
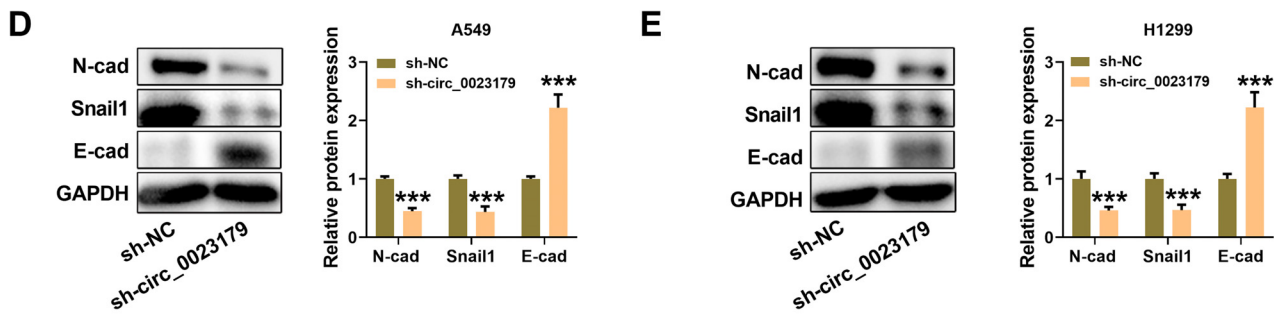158
www.biomolbiomed.com

Figure 2. (Continued) Biological characteristics of circ_0023179 in NSCLC cells. (A) qRT-PCR was used to verify the transfection efficiency of two stably transfected cell lines, A549-sh-circ_0023179 and H1299-sh-circ_0023179; (B) Colony formation assays were used to assess the effect of circ_0023179 knockdown on the proliferation ability of NSCLC cells; (C) EdU assays were used to evaluate the proliferation ability of two stably transfected cell lines, A549-sh-circ_0023179 and H1299-sh-circ_0023179; (D and E) Western blot assays were used to detect EMT-related proteins. *$P < 0.05$, **$P < 0.01$, ***$P < 0.001$. NSCLC: Non-small-cell lung cancer; qRT-PCR: Quantitative real-time polymerase chain reaction; EMT: Epithelial–mesenchymal transition.
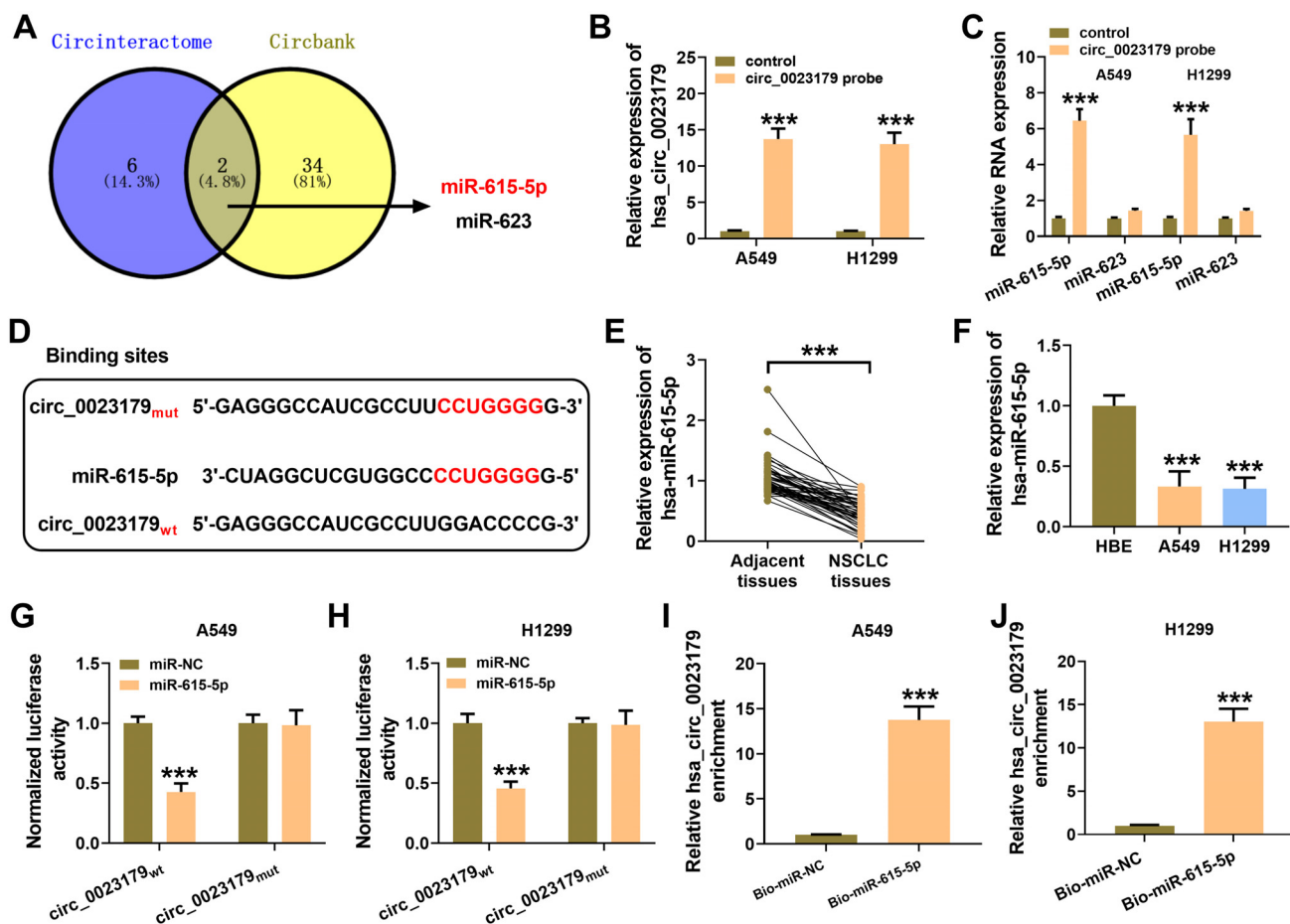

Figure 3. circ_0023179 targeted miR-615-5p. (A) The circInteractome and circbank biology websites were used to predict the target miRNAs for circ_0023179; (B and C) A549 and H1299 cells were examined using a circ_0023179 probe in RIP assays; (D) The binding site of circ_0023179 for miR-615-5p was predicted; (E) qRT-PCR was used to detect the expression of miR-615-5p in NSCLC tissues and paraneoplastic tissues; (F) qRT-PCR was used to detect the expression of miR-615-5p in the HBE, A549, and H1299 cells; (G and H) Dual-luciferase reporter assays were used to verify the binding of circ_0023179 and miR-615-5p; (I and J) RNA pull-down assays were used for the biotin-labeled miR-615-5p in A549 and H1299 cells. *$P < 0.05$, **$P < 0.01$, ***$P < 0.001$. miRNA: MicroRNA; RIP: RNA immunoprecipitation; qRT-PCR: Quantitative real-time polymerase chain reaction; NSCLC: Non-small-cell lung cancer.

MiR-615-5p inhibitor inverted the regulative effect of sh-circ_0023179 on NSCLC cells

First, miR-615-5p was knocked down and introduced into A549 and H1299 cells. qRT-PCR was used to assess the knockdown efficiency (see Figure 4A and 4B). Next, anti-miR-615-5p was transfected into A549-sh-circ_0023179 and H1299-sh-circ_0023179 cell lines. Plate-clone formation and EdU assay results showed that anti-miR-615-5p promoted
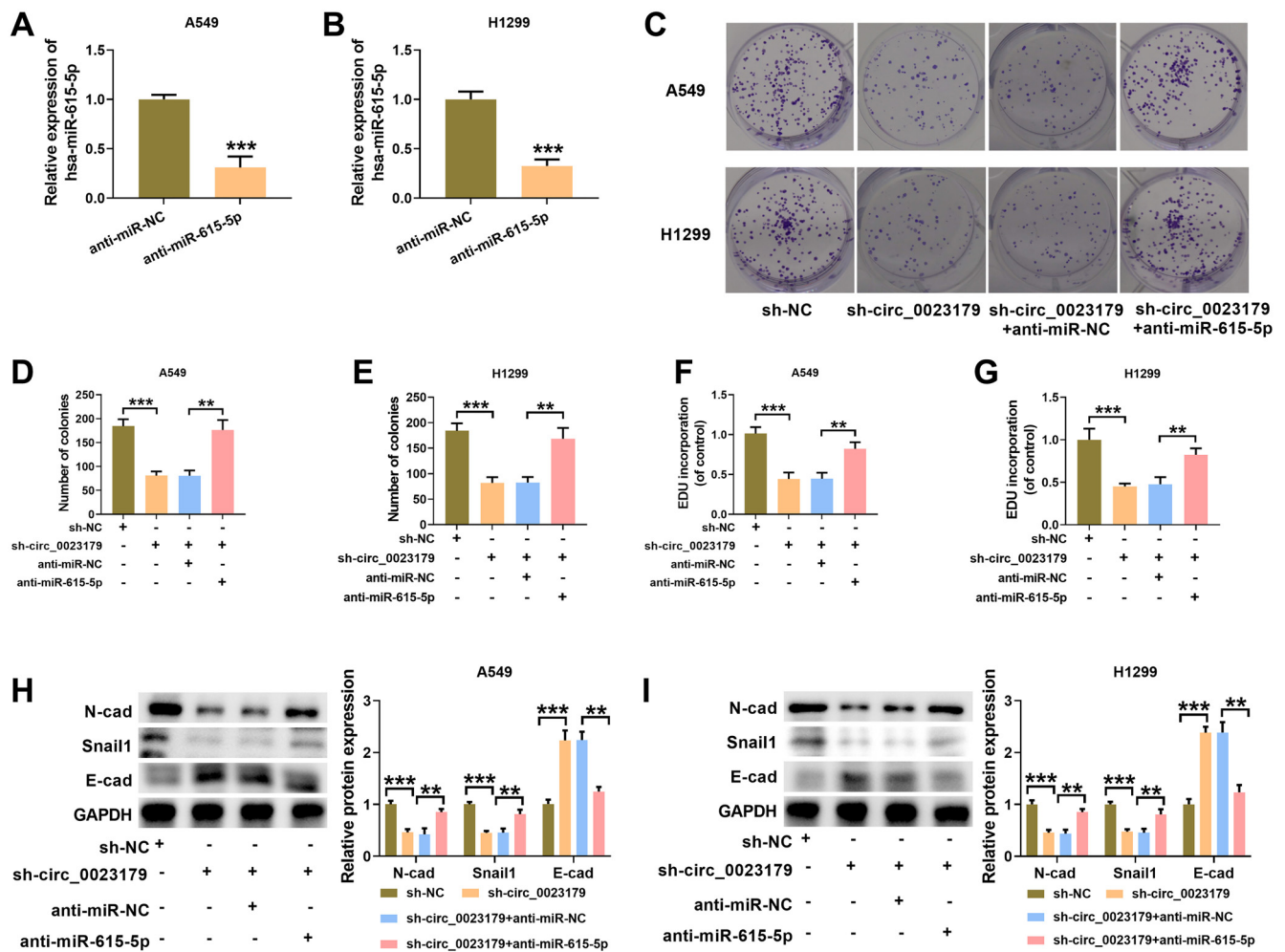
Guo et al.
circ_0023179 modulates NSCLC
159
www.biomolbiomed.com

Figure 4. Anti-miR-615-5p attenuated the inhibitory effect of sh-circ_0023179 on the proliferation of NSCLC cells. (A and B) qRT-PCR was used to verify the knockdown efficiency of miR-615-5p in NSCLC cells; (C–E) Colony formation assays were used to detect the number of cell clones; (F and G) EdU assays were used to assess cell proliferation efficiency; (H and I) Western blot was used to detect EMT-related marker proteins. $*P < 0.05$, $**P < 0.01$, $***P < 0.001$. NSCLC: Non-small-cell lung cancer; qRT-PCR: Quantitative real-time polymerase chain reaction; EMT: Epithelial–mesenchymal transition.

the proliferation of A549-sh-circ_0023179 and H1299-sh-circ_0023179 cells (see Figure 4C–4G). Additionally, the knockdown of miR-615-5p in A549-sh-circ_0023179 and H1299-sh-circ_0023179 cells increased the levels of EMT-related markers N-cad and Snail1, and decreased E-cad levels in both cell lines (see Figure 4H and 4I).

MiR-615-5p targeted CDH3
CDH3 was predicted to be a downstream target of miR-615-5p by four bioinformatics sites; the predicted binding sites for CDH3 and miR-615-5p are shown in Figure 5A and 5B. Notably, Figure 5C and 5D shows high expression of CDH3 in NSCLC tissues. Additionally, CDH3 expression was higher in NSCLC cells compared to HBE cells (see Figure 5E and 5F). The results showed that miR-615-5p mimics could bind the CDH3 3′UTR sequence, leading to decreased luciferase activity (see Figure 5G and 5H). The overexpression of miR-615-5p suppressed CDH3 expression in NSCLC cells (see Figure 5I and 5J).

Overexpression of CDH3 attenuated the proliferation inhibitory effect of circ_0023179 knockdown on NSCLC cells
The knockdown of miR-615-5p in A549-sh-circ_0023179 and H1299-sh-circ_0023179 cells significantly increased CDH3 expression (see Figure 6A and 6B). Similarly, CDH3 levels were restored in A549-sh-circ_0023179 and H1299-sh-circ_0023179 cells by the overexpression of CDH3 (see Figure 6C and 6D). Additionally, the effect of sh-circ_0023179 on NSCLC cell growth was significantly mitigated by the overexpression of CDH3 (see Figure 6E–6H). The detection of EMT-related marker proteins revealed that the effects of silencing circ_0023179 on N-cad, Snail1, and E-cad proteins in NSCLC cells were reversed by the overexpression of CDH3 (see Figure 6I and 6J).

Sh-Circ_0023179 inhibited NSCLC tumor growth
In addition to in vitro assays, A549-sh-circ_0023179 cells were inoculated subcutaneously in nude mice to construct a nude mouse subcutaneous tumor model for in vivo experiments. The results showed that sh-circ_0023179 reduced tumor volume and
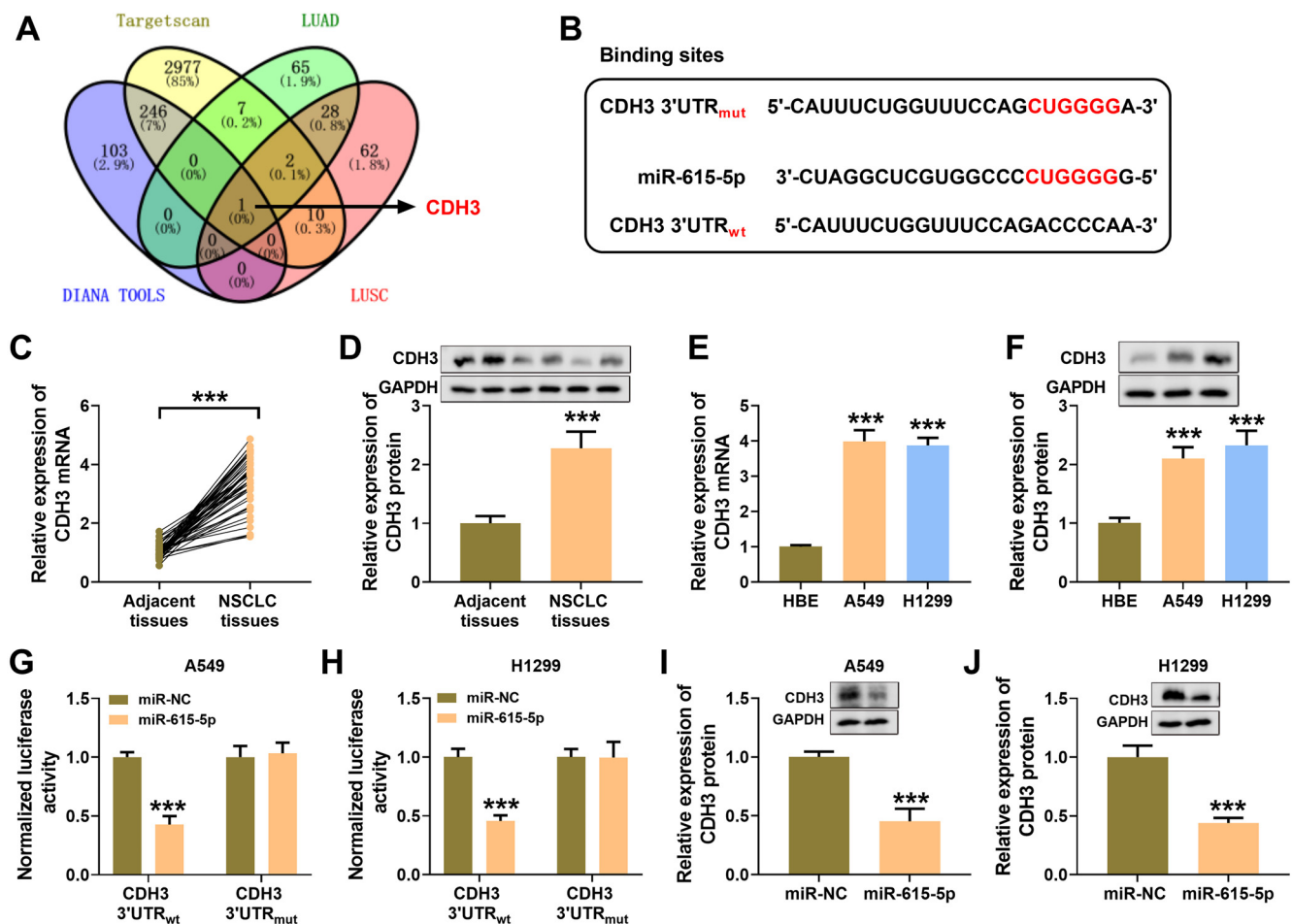
Guo et al.
circ_0023179 modulates NSCLC
160
www.biomolbiomed.com

Figure 5. CDH3 was a downstream gene of miR-615-5p. (A) Four bioinformatic sites (i.e., targetscan, LUAD, DINAN TOOLS, and LUSC) were used to predict the potential target mRNA of miR-615-5p; (B) The binding sites of miR-615-5p to CDH3; (C) qRT-PCR was used to detect CDH3 expression in the paraneoplastic and NSCLC tissues; (D) Western blot was used to detect the expression of CDH3 protein in the paraneoplastic and NSCLC tissues; (E) qRT-PCR was used to detect the expression of CDH3 in HBE, A549, and H1299 cells; (F) Western blot was used to detect CDH3 protein expression in HBE, A549, and H1299 cells; (G and H) Dual-luciferase reporter assays were used to verify the binding of CDH3 mRNA and miR-615-5p; (I and J) Western blot assay was used to examine the effect of miR-615-5p on CDH3 protein expression in A549 and H1299 cells. $*P < 0.05$, $**P < 0.01$, $***P < 0.001$. CDH3: Cadherin 3; mRNA: Messenger RNA; qRT-PCR: qRT-PCR: Quantitative real-time polymerase chain reaction; HBE: Human bronchial epithelial.

weight in NSCLC (see Figure 7A and 7B). Western blot assay results showed that silencing circ_0023179 inhibited N-cad and Snail1 protein levels and upregulated E-cad protein content in the tumor tissues (see Figure 7C). IHC assay results showed that sh-circ_0023179 markedly reduced Ki-67 content in tumors (see Figure 7D).

Discussion

In this study, the effects of circ_0023179 on NSCLC were investigated both in vitro and in vivo. Circ_0023179 regulates the proliferation, apoptosis, and EMT processes of NSCLC cells through the miR-615-5p/CDH3 axis. NSCLC is a malignant tumor, and although existing treatments have shown some efficacy, patient prognosis remains poor [24]. The study identified circ_0023179 as a potential biomarker for NSCLC [9].

Recent research has shown that circRNAs are robust against RNases and are present in various tissues and body fluids,

resulting in a longer half-life and greater stability. This stability suggests that circRNAs may serve as diagnostic or predictive biomarkers for various cancers [25]. For example, serum levels of circ-FAF1 and circ-ELP3 have been proposed as novel potential biomarkers for breast cancer diagnosis [26]. In gastric cancer patients, a low level of hsa:circ_0001811 indicates a better prognosis [27]. Additionally, circRNAs have been implicated in cancer genesis and pathogenesis; for instance, hsa:circ_0005273 has been shown to promote breast cancer tumorigenesis by sponging miR-200a-3p to upregulate YAP1, thereby affecting the Hippo pathway [28]. In this study, the knockdown of circ_0023179 in NSCLC inhibited the proliferative capacity of NSCLC cells by suppressing the EMT process.

Available data suggest that circRNAs may play a crucial role in the onset and progression of various human diseases [29]. To date, most research on circRNAs has focused on their function as miRNA sponges or competitive endogenous RNAs [25].
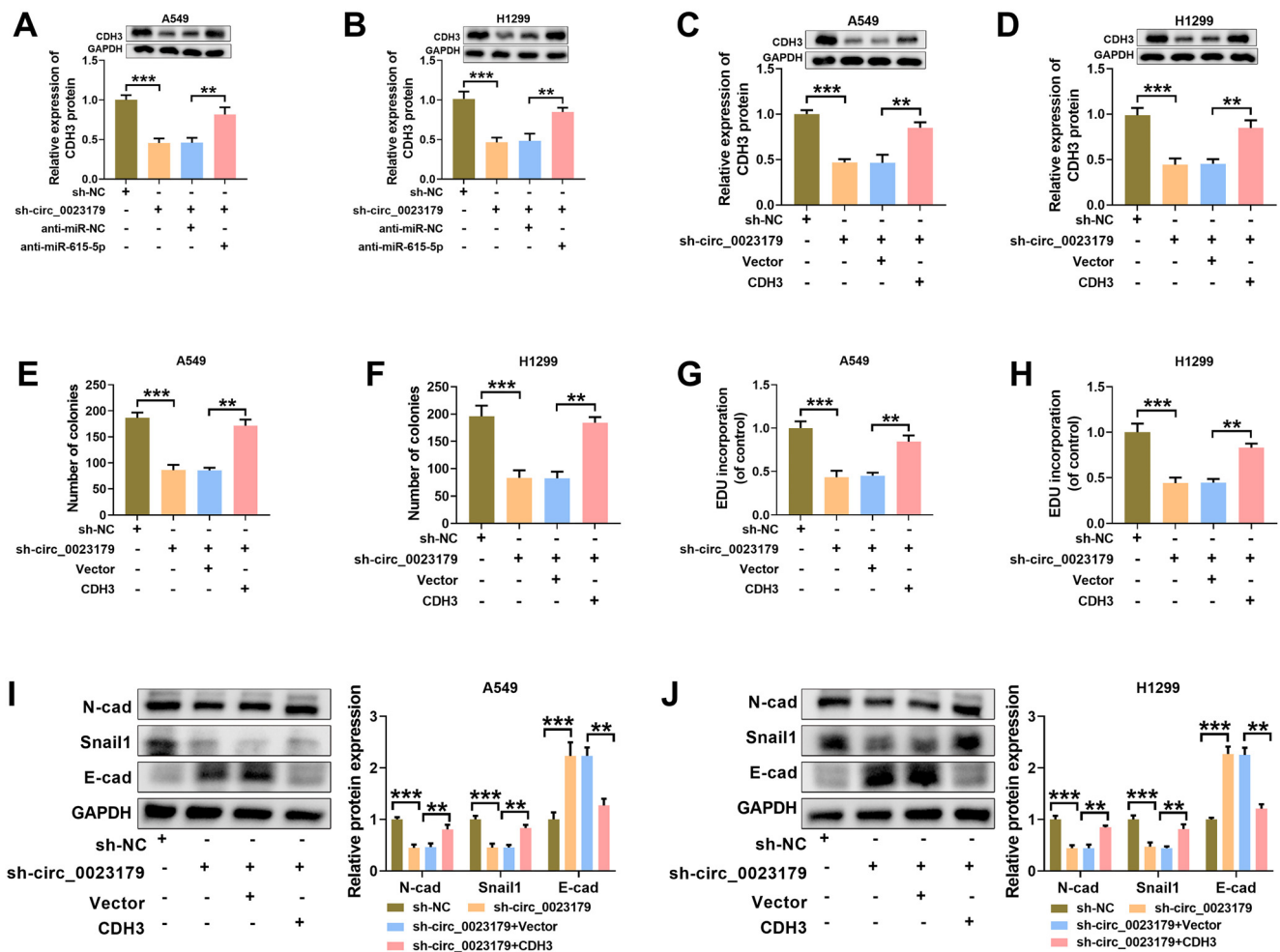
Guo et al.
circ_0023179 modulates NSCLC
161
www.biomolbiomed.com

Figure 6. The overexpression of CDH3 improved the inhibitory effect of sh-circ_0023179 on the proliferation of NSCLC cells. (A and B) Circ_0023179 and miR-615-5p were both knocked down in A549 and H1299 cells, and western blot was used to detect CDH3 protein expression; (C and D) Western blot was used to detect CDH3 protein expression after the knockdown of circ_0023179 and the overexpression of CDH3 in A549 and H1299 cells; (E and F) Colony formation assays were used to detect the number of cell clones; (G and H) EdU assays were used to examine cell proliferation efficiency; (I and J) Western blot assays were used to detect the EMT-related marker proteins. *$P < 0.05$, **$P < 0.01$, ***$P < 0.001$. CDH3: Cadherin 3; NSCLC: Non-small-cell lung cancer; EMT: Epithelial–mesenchymal transition.

CircRNAs containing miRNA response elements are primarily located in the cytoplasm and can negate the inhibitory effects of miRNAs on downstream targets by binding to complementary miRNA sequences [30]. This study investigated whether miR-615-5p binds to circ_0023179. Previous studies have shown that miR-615-5p functions as a tumor suppressor in several cancers, including HCC, prostate cancer, and nasopharyngeal carcinoma [12, 31, 32]. In this study, miR-615-5p was found to be lowly expressed in NSCLC. The knockdown of circ_0023179 led to elevated miR-615-5p levels, which reversed the inhibitory effect of sh-circ_0023179 on NSCLC cell proliferation, suggesting that miR-615-5p may also suppress cancer cell proliferation in NSCLC.

CircRNAs function by adsorbing and degrading miRNAs to increase mRNA levels of target genes, binding and regulating protein functions, or influencing epigenetic modifications, thereby directly regulating the expression of homologous genes [29]. In this study, we identified CDH3 as a downstream

target of miR-615-5p through multiple databases. CDH3, a member of the cadherin family, was originally discovered in 1986 by Nose and Takeichi [33] in mouse embryonic development. This family constitutes an essential category of intercellular adhesion molecules involved in regulating cell polarity and differentiation, contributing to the maintenance of tissue homeostasis [34–36]. In normal human tissues, CDH3 expression is low, detected primarily in the thymus and fetal brain. However, high expression levels of CDH3 have been observed in various human tumor tissues [37]. Research has also shown that CDH3 promotes tumorigenesis in gastric cancer, pancreatic cancer, and breast cancer, while it inhibits tumorigenesis in HCC and melanoma [38–40]. Our results demonstrated that the knockdown of circ_0023179 increased miR-615-5p expression and decreased CDH3 expression, suggesting that circ_0023179 promotes the EMT process in NSCLC cells through the miR-615-5p/CDH3 axis, thereby enhancing cell proliferation.
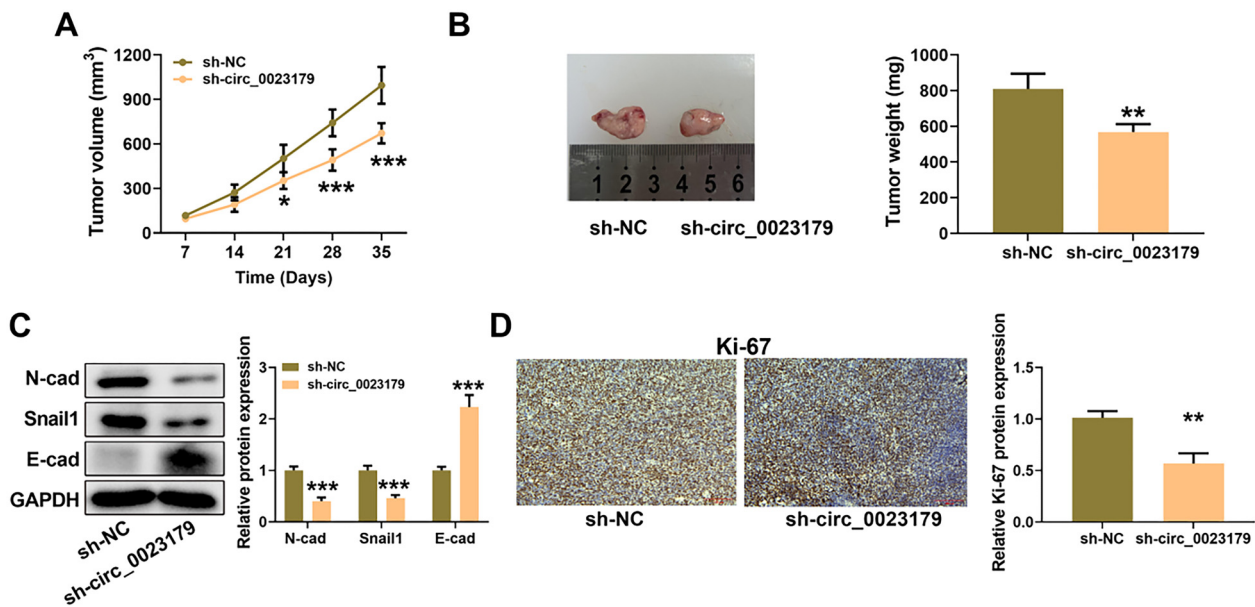
Guo et al.
circ_0023179 modulates NSCLC
162
www.biomolbiomed.com

Figure 7. **sh-circ_0023179 inhibited NSCLC tumor growth the A549-sh-circ_0023179 cells were inoculated subcutaneously in nude mice.** (A) Tumor size was measured once a week; (B) Tumors were weighed once a week; (C) Western blot was used to detect EMT-related protein expression in tumor tissues; (D) IHC staining was used to detect the Ki-67 protein index. $*P < 0.05$, $**P < 0.01$, $***P < 0.001$. NSCLC: Non-small-cell lung cancer; EMT: Epithelial–mesenchymal transition; IHC: Immunohistochemical.

Conclusion

This study revealed that circ_0023179 increases CDH3 levels by sponging miR-615-5p, facilitating the EMT process and enhancing cell proliferation in NSCLC cells. These findings suggest that circ_0023179 could be a strategic target for the prospective diagnosis and treatment of NSCLC.

Conflicts of interest: Authors declare no conflicts of interest.

Data availability: The data supporting the findings of this study can be obtained from the corresponding author, upon request.

References

[1] Salehi M, Movahedpour A, Tayarani A, Shabaninejad Z, Pourhanifeh MH, Mortezapour E, et al. Therapeutic potentials of curcumin in the treatment of non-small-cell lung carcinoma. Phytother Res 2020;34(10):2557–76. https://doi.org/10.1002/ptr.6704.

[2] Tan S, Sun D, Pu W, Gou Q, Guo C, Gong Y, et al. Circular RNA F-circEA-2a derived from EML4-ALK fusion gene promotes cell migration and invasion in non-small cell lung cancer. Mol Cancer 2018;17(1):138. https://doi.org/10.1186/s12943-018-0887-9.

[3] Gridelli C, Rossi A, Carbone DP, Guarize J, Karachaliou N, Mok T, et al. Non-small-cell lung cancer. Nat Rev Dis Primers 2015;1:15009. https://doi.org/10.1038/nrdp.2015.9.

[4] Danan M, Schwartz S, Edelheit S, Sorek R. Transcriptome-wide discovery of circular RNAs in Archaea. Nucl Acids Res 2012;40(7):3131–42. https://doi.org/10.1093/nar/gkr1009.

[5] Arnaiz E, Sole C, Manterola L, Iparraguirre L, Otaegui D, Lawrie CH. CircRNAs and cancer: biomarkers and master regulators. Semin Cancer Biol 2019;58:90–9. https://doi.org/10.1016/j.semcancer.2018.12.002.

[6] Di X, Jin X, Li R, Zhao M, Wang K. CircRNAs and lung cancer: biomarkers and master regulators. Life Sci 2019;220:177–85. https://doi.org/10.1016/j.lfs.2019.01.055.

[7] Chen C, Zhang M, Zhang Y. Circ_0000079 Decoys the RNA-binding protein FXR1 to interrupt formation of the FXR1/PRCKI complex and decline their mediated cell invasion and drug resistance in NSCLC. Cell Transplant 2020;29:963689720961070. https://doi.org/10.1177/0963689720961070.

[8] Wang J, Li H. CircRNA circ_0067934 silencing inhibits the proliferation, migration and invasion of NSCLC cells and correlates with unfavorable prognosis in NSCLC. Eur Rev Med Pharmacol Sci 2018;22(10):3053–60. https://doi.org/10.26355/eurrev_201805_15063.

[9] Zhang Q, Qin S, Peng C, Liu Y, Huang Y, Ju S. Circulating circular RNA hsa:circ_0023179 acts as a diagnostic biomarker for non-small-cell lung cancer detection. J Cancer Res Clin Oncol 2022;149:3649–60. https://doi.org/10.1007/s00432-022-04254-0.

[10] Croce CM, Calin GA. miRNAs, cancer, and stem cell division. Cell 2005;122(1):6–7. https://doi.org/10.1016/j.cell.2005.06.036.

[11] Rahmoon MA, Youness RA, Gomaa AI, Hamza MT, Waked I, El Tayebi H M, et al. MiR-615-5p depresses natural killer cells cytotoxicity through repressing IGF-1R in hepatocellular carcinoma patients. Growth Factors 2017;35(2–3):76–87. https://doi.org/10.1080/08977194.2017.1354859.

[12] Wu X, Deng L, Tang D, Ying G, Yao X, Liu F, et al. miR-615-5p prevents proliferation and migration through negatively regulating serine hydromethyltransferase 2 (SHMT2) in hepatocellular carcinoma. Tumor Biol 2016;37(5):6813–21. https://doi.org/10.1007/s13277-015-4506-8.

[13] Li Y, Zhang M, Li X, Wang Y, Wang Y, Li Y, et al. Hydroxyacid oxidase 2 (HAO2) inhibits the tumorigenicity of hepatocellular carcinoma and is negatively regulated by miR-615-5p. J Immunol Res 2022;2022:5003930. https://doi.org/10.1155/2022/5003930.

[14] Wu M, Kong C, Cai M, Huang W, Chen Y, Wang B, et al. Hsa:circRNA_002144 promotes growth and metastasis of colorectal cancer through regulating miR-615-5p/LARP1/mTOR pathway. Carcinogenesis 2021;42(5):601–10. https://doi.org/10.1093/carcin/bgaa140.

[15] Chen L, Nan A, Zhang N, Jia Y, Li X, Ling Y, et al. Circular RNA 100146 functions as an oncogene through direct binding to miR-361-3p and

miR-615-5p in non-small cell lung cancer. Mol Cancer 2019;18(1):13. https://doi.org/10.1186/s12943-019-0943-0.

[16] Li D, Yan L, Zhang J, Gu F. Circular RNA hsa:circ_0004396 acts as a sponge of miR-615-5p to promote non-small cell lung cancer progression and radioresistance through the upregulation of P21-Activated Kinase 1. J Clin Lab Anal 2022;36(6):e24463. https://doi.org/10.1002/jcla.24463.

[17] Zhang M, Lin B, Liu Y, Huang T, Chen M, Lian D, et al. LINC00324 affects non-small cell lung cancer cell proliferation and invasion through regulation of the miR-139-5p/IGF1R axis. Mol Cell Biochem 2020;473(1–2):193–202. https://doi.org/10.1007/s11010-020-03819-2.

[18] Vieira AF, Paredes J. P-cadherin and the journey to cancer metastasis. Mol Cancer 2015;14:178. https://doi.org/10.1186/s12943-015-0448-4.

[19] Zhou Y, Chi Y, Bhandari A, Xia E, Thakur PC, Qu J, et al. Downregulated CDH3 decreases proliferation, migration, and invasion in thyroid cancer. Am J Transl Res 2020;12(6):3057–67. https://pubmed.ncbi.nlm.nih.gov/32655830/..

[20] Siret C, Dobric A, Martirosyan A, Terciolo C, Germain S, Bonier R, et al. Cadherin-1 and cadherin-3 cooperation determines the aggressiveness of pancreatic ductal adenocarcinoma. Br J Cancer 2018;118(4):546–57. https://doi.org/10.1038/bjc.2017.411.

[21] Li L, Yu S, Wu Q, Dou N, Li Y, Gao Y. KLF4-Mediated CDH3 upregulation suppresses human hepatoma cell growth and migration via GSK-3beta signaling. Int J Biol Sci 2019;15(5):953–61. https://doi.org/10.7150/ijbs.30857.

[22] Nie X, Liu H, Ye W, Wei X, Fan L, Ma H, et al. LRP5 promotes cancer stem cell traits and chemoresistance in colorectal cancer. J Cell Mol Med 2022;26(4):1095–112. https://doi.org/10.1111/jcmm.17164.

[23] Wang Y, Zhang Y, Fang M, Bao W, Deng D. Two novel susceptibility loci for non-small cell lung cancer map to low-density lipoprotein receptor-related protein 5. Oncol Lett 2016;12(4):2307–18. https://doi.org/10.3892/ol.2016.4954.

[24] Mithoowani H, Febbraro M. Non-small-cell lung cancer in 2022: a review for general practitioners in oncology. Curr Oncol (Toronto, Ont) 2022;29(3):1828–39. https://doi.org/10.3390/curroncol29030150.

[25] Memczak S, Jens M, Elefsinioti A, Torti F, Krueger J, Rybak A, et al. Circular RNAs are a large class of animal RNAs with regulatory potency. Nature 2013;495(7441):333–8. https://doi.org/10.1038/nature11928.

[26] Omid-Shafaat R, Moayeri H, Rahimi K, Menbari MN, Vahabzadeh Z, Hakhamaneshi MS, et al. Serum Circ-FAF1/Circ-ELP3:A novel potential biomarker for breast cancer diagnosis. J Clin Lab Anal 2021;35(11):e24008. https://doi.org/10.1002/jcla.24008.

[27] Zhang H, Li Z, Ruan Y, Sun W, Yu R. Low expression of hsa:circ_0001811 in gastric cancer and its role in clinical diagnosis. J Clin Lab Anal 2021;35(2):e23642. https://doi.org/10.1002/jcla.23642.

[28] Wang X, Ji C, Hu J, Deng X, Zheng W, Yu Y, et al. Hsa:circ_0005273 facilitates breast cancer tumorigenesis by regulating YAP1-hippo sig-

naling pathway. J Exp Clin Cancer Res 2021;40(1):29. https://doi.org/10.1186/s13046-021-01830-z.

[29] Lu Y, Li K, Gao Y, Liang W, Wang X, Chen L. CircRNAs in gastric cancer: current research and potential clinical implications. FEBS Lett 2021;595(21):2644–54. https://doi.org/10.1002/1873-3468.14196.

[30] Hansen TB, Jensen TI, Clausen BH, Bramsen JB, Finsen B, Damgaard CK, et al. Natural RNA circles function as efficient microRNA sponges. Nature 2013;495(7441):384–8. https://doi.org/10.1038/nature11993.

[31] Zeng L, Liu YM, Yang N, Zhang T, Xie H. Hsa:circRNA_100146 promotes prostate cancer progression by upregulating TRIP13 via sponging miR-615-5p. Front Mol Biosci 2021;8:693477. https://doi.org/10.3389/fmolb.2021.693477.

[32] Tang L, Xiong W, Zhang L, Wang D, Wang Y, Wu Y, et al. circSETD3 regulates MAPRE1 through miR-615-5p and miR-1538 sponges to promote migration and invasion in nasopharyngeal carcinoma. Oncogene 2021;40(2):307–21. https://doi.org/10.1038/s41388-020-01531-5.

[33] Nose A, Takeichi M. A A novel cadherin cell adhesion molecule: its expression patterns associated with implantation and organogenesis of mouse embryos. J Cell Biol 1986;103(6 Pt 2):2649–58. https://doi.org/10.1083/jcb.103.6.2649.

[34] Loh CY, Chai JY, Tang TF, Wong WF, Sethi G, Shanmugam MK, et al. The E-Cadherin and N-cadherin switch in epithelial-to-mesenchymal transition: signaling, therapeutic implications, and challenges. Cells 2019;8(10):1118. https://doi.org/10.3390/cells8101118.

[35] Mendonsa AM, Na TY, Gumbiner BM. E-cadherin in contact inhibition and cancer. Oncogene 2018;37(35):4769–80. https://doi.org/10.1038/s41388-018-0304-2.

[36] Padmanaban V, Krol I, Suhail Y, Szczerba BM, Aceto N, Bader JS, et al. E-cadherin is required for metastasis in multiple models of breast cancer. Nature 2019;573(7774):439–44. https://doi.org/10.1038/s41586-019-1526-3.

[37] Na TY, Schecterson L, Mendonsa AM, Gumbiner BM. The functional activity of E-cadherin controls tumor cell metastasis at multiple steps. Proc Natl Acad Sci U S A 2020;117(11):5931–7. https://doi.org/10.1073/pnas.1918167117.

[38] Sridhar S, Rajesh C, Jishnu PV, Jayaram P, Kabekkodu SP. Increased expression of P-cadherin is an indicator of poor prognosis in breast cancer: a systematic review and meta-analysis. Breast Cancer Res Treat 2020;179(2):301–13. https://doi.org/10.1007/s10549-019-05477-5.

[39] Dobritoiu M, Stepan AE, Margaritescu C, Simionescu CE, Vere CC, Schenker M, et al. Immunoexpression of E-cadherin, P-cadherin and fibronectin in gastric carcinomas. Rom J Morphol Embryol 2019;60(2):573–9. https://pubmed.ncbi.nlm.nih.gov/31658331/..

[40] Subbiah V, Erwin W, Mawlawi O, Mccoy A, Wages D, Wheeler C, et al. Phase I study of P-cadherin-targeted radioimmunotherapy with (90)Y-FF-21101 monoclonal antibody in solid tumors. Clin Cancer Res 2020;26(22):5830–42. https://doi.org/10.1158/1078-0432.CCR-20-0037.

Related articles

1. Mechanism of OTUD5 in non-small cell lung cancer cell proliferation, invasion, and migration

   Xuebing Li et al., BJBMS, 2022

2. Role of FBXW7 in the quiescence of gefitinib-resistant lung cancer stem cells in EGFR-mutant non-small cell lung cancer

   Moulid Hidayat et al., BJBMS, 2019

3. Long non-coding RNA PVT1 regulates the migration of hepatocellular carcinoma HepG2 cells via miR-3619-5p/MKL1 axis

   Hua Liu et al., BJBMS, 2020